Multifractal Analysis of Histopathological Tissue Images

ChiangHau, TAY
Computer Science and Software Engineering
University of Canterbury
Christchurch, New Zealand
cht27@uclive.ac.nz

Ramakrishnan, MUKUNDAN
Computer Science and Software Engineering
University of Canterbury
Christchurch, New Zealand
mukund@cosc.canterbury.ac.nz

Daniel, RACOCEANU
Image & Pervasice Access Lab
Agency for Science, Technology and Research
Singapore
Daniel.racoceanu@ens2m.fr

Abstract— **Histopathological classification and grading of biopsy specimens play an important role in early cancer detection and prognosis. Nottingham scoring system is one of the standard grading procedures used in breast cancer assessment, where three parameters, Mitotic Count (MC), Nuclear Pleomorphism (NP), and Tubule Formation (TF) are used for prognostic information. The grading takes into account the deviations in cellular structures and appearance from normal, using measures such as density, size, colour and regularity. Cell structures in tissue images are also known to exhibit multifractal characteristics. This paper looks at the multifractal properties of several graded biopsy specimens and analyses the dependency and variation of the fractal parameters with respect to the scores assigned by pathologists.**

Keywords-Breast cancer assessment; Multifractal spectra; Image analysis; Histopathologic classification; Feature detection; Cancer grading

I. INTRODUCTION

According to the statistics collected by the International Agency for Research on Cancer (IARC), breast cancer is the most frequent cancer women [1]. By comparing the breast cancer with other types of cancers, it is ranked as the fifth major cause of death. However, breast cancer is still the deadliest cancer in several developing and developed countries. As in most diseases, early diagnosis and medical treatment is the key for recovery. Histopathological classification and grading of biopsy samples provide valuable prognostic information that could be used for diagnosis and treatment. Nottingham scoring system is the standard for breast cancer grading. It focuses on three criteria (1) Mitosis Count (MC), (2) Nuclear Pleomorphism (NP), and (3) Tubule Formation (TF) [2], [3].

The current procedure for breast cancer grading is manually performed by the pathologists. Breast tissue samples of a patient are taken and examined under the microscope, and grades assigned based on the deviation of cell structures from normal tissues. This is a time consuming process [4]. Histopathological images are now available in high resolution and high magnification digital formats, which can be further processed to extract several structural information useful to pathologists.

The grading of biopsy samples is essentially based on the deviation of cell structures from the normal tissue. Cell structures also have multifractal characteristics that could be directly used for identifying pathological conditions. Therefore, it would be useful to explore the relationship between various multifractal measures of cell structures in tissues and the corresponding pleomorphic scores assigned by pathologists. This paper proposes an approach using local intensity variations in images to identify mitotic cells and also to obtain an estimate of the NP and TF scores based on the multifractal spectra computed from the images.

II. RELATED WORK

Several algorithms for automatic breast cancer grading have been proposed in literature. However, most of the methods can only handle one of the three Nottingham criteria. Tutac et al. [6] and Dalle et al. [7] have recently developed methods for automatic indexing and grading of histopathological images including all three parameters. Petushi et al. have also discussed the multi-resolution method which combines all the criteria in their papers [8], [9].

A method of counting the mitotic cells is proposed by Baak et al. [10], [11]. Segmentation of mitotic cells is based on intensity thresholding and region growing techniques. Traditional colour based algorithms including thresholding, morphological operation, watershed algorithm, etc, are proposed in [12], [13], [14], [15], and [16]. Dalle et al. proposed a method for selecting critical cell nuclei for nuclear pleomorphism scoring [17]. They have shown that the proposed concept requires less computational time and provides accurate classification results. A method for analysing tubule formation is proposed by Petushi et al. [8], [9]. In their research, the microstructure of the histological image is presented. Localised tubular formations can be obtained by segmentation and classification of the cells.

Multifractal formalism is an effective tool for biomedical image processing. Segmentation, classification, signal analysis, etc using multifractal have been proposed by several authors [18]-[24]. Multifractal analysis has recently been used in the domain of medical image processing [19], [21]. The statistical characterisation of the intensity variations in an image structure

can be represented by the multifractal spectrum. Despite the complexity of highly irregular shape of the tissue and cell images, multifractal analysis can resolve the local densities and represent the statistical properties of shapes with complex spatial arrangements.

III. MULTIFRACTAL ANALYSIS

Holder exponent or the local singularity coefficient α, describes the local variation of an intensity based measure within the neighbourhood of a pixel. The measure function is denoted as $\mu_p(w)$ where w is the size of a square region (window) centred at a pixel shown in Fig. 1(a). The variation of the intensity measure with respect to w can be characterised as follows:

$$\mu_p(w) = Cw^{\alpha_p} \qquad (1)$$

$$w = 2i + 1, \quad i = 0,1,2,\dots,m \qquad (2)$$

$$a_p = \frac{\log(\mu)}{\log(w)} \qquad (3)$$

where C is an arbitrary constant. In (2), m is the total number of windows used in the computation of α_p. The value of α_p at each pixel is given by (3), and is estimated from the slope of the linear regression line in a log-log plot where $\log(\mu)$ is plotted against $\log(w)$.

The four commonly used intensity measures in multifractal analysis are (1) maximum measure, (2) inverse-minimum measure, (3) summation measure, and (4) iso measure [18], [19], [23], [24]. The intensity range of the image is assumed to be distributed from 0 to 1. Maximum measure evaluates the maximum intensity of the pixels in w. The inverse minimum measure uses the minimum intensity value subtracted from one. The summation measure computes the total intensity value; and iso counts the number of nearby pixels which have a similar value as the centre pixel.

The second stage of multifractal analysis is the calculation of the fractal dimension of sets of points having the same singularity coefficient α. The fractal dimension is denoted as $f(\alpha)$ in (4). The variation of $f(\alpha)$ with α is known as the multifractal spectrum. As shown in Fig. 1(b), the fractal dimension of the image of size N by N pixels can be calculated via the box counting method [25], [26]. Box counting is a method that counts the number of boxes, $n(\varepsilon)$ with size ε, that contain pixels with an α-value within the α-interval $[\alpha_i, \alpha_{i+1}]$. The α-intervals are obtained by subdividing the range of α-values into a pre-specified number of subintervals.

$$f(\alpha) = \frac{\log n(\varepsilon)}{\log \varepsilon} \qquad (4)$$

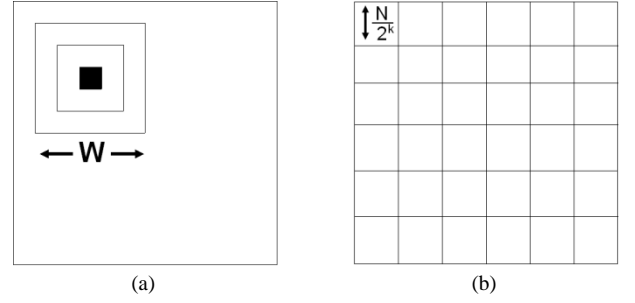$$\varepsilon = \frac{N}{2^k}, \quad k \le \frac{\log N}{\log 2} \qquad (5)$$

Figure 1. (a) Computation of Holder Exponent, α. (b) box counting

IV. METHODS

The system overview for the multifractal analysis of breast cancer sections is indicated in Fig. 2. The high resolution high magnification histopathological images are sub-divided into small image frames of size 288 x 288 pixels. Each image frame contains a border of 16 pixels wide, which is also the window size for measuring local singularity coefficient α. The system calculates the α-value at each pixel position.

An α-threshold comparison is applied to separate the sub-image frames that contain epithelial type tissues from those containing non-epithelial type tissues. Huang et al. use epithelial tissue images to extract information on Nottingham parameters in their paper [26]. The process of selecting epithelial tissue images is presented in the next section. After that the system detects the mitosis cells and computes fractal spectrum of the epithelial sub-image frames. The mitotic cell detection is a method which is based on the computed α-values within the cell region. We then explore if the NP and TF scores can be estimated from the multifractal spectrum.
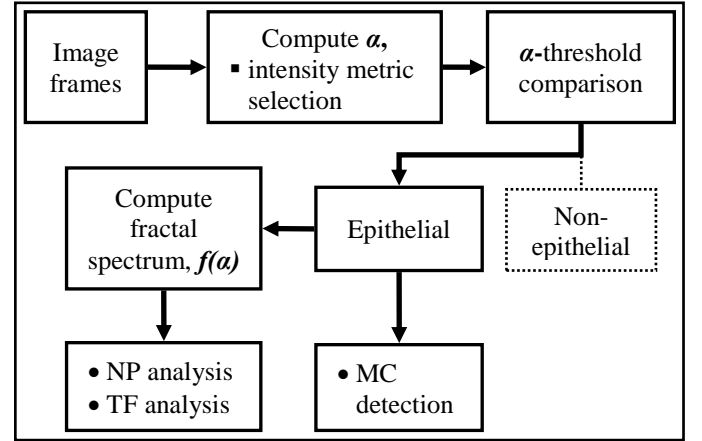

Figure 2. System overview of multifractal analysis of tissue images

A. First Stage Classification Process

Unlike the classification methods presented in [8] and [9], the proposed method given in Fig. 2 separates the image frames into two tissue structure categories, which are (1) non-epithelial type and (2) epithelial type. Examples of these types of images are given in Fig. 3. Stroma and fat-like tissues have plain tissue substance, and they are irrelevant to the breast grading. Hence these are classified as non-epithelial group and are separated out during the first stage selection process.

Based on the multifractal properties of the sub-images, the characteristic of the cell nuclei can be indentified via the α-range of the (1) maximum measure and (2) summation measure and the minimum α-value in the (3) iso measure.

As indicated in Table I, the epithelial tissues have larger difference in α-max and α-min (α-range) of the α-image than the non-epithelial in both maximum measure and summation measure. The epithelial tissue contains nuclei cells along with other tissue substances; hence, its intensity distribution is richer than the stroma and fat-like tissue image. It contains variations of α-value in the α-image; therefore, its α-range is larger than non-epithelial type. The minimum α-value of epithelial tissue is smaller than the non-epithelial type because these types of tissues have nearly uniform intensity distribution and yield higher values for the iso measure.
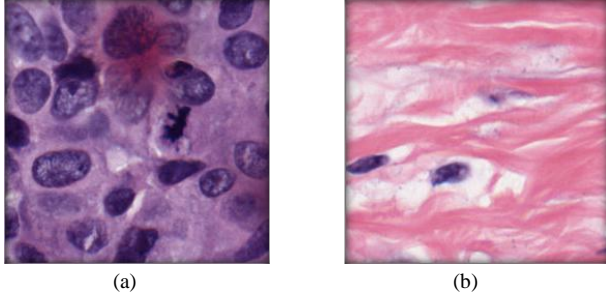

(a)   (b)

Figure 3.   Tissue image example of (a) epithelial type (b) non-epithelial type

TABLE I.   TABLE FOR CLASSIFICATION

Type of multifractal	Epithelial	
	α-min	α-max
maximum measure	[0]	[0.37, 0.94]
summation measure	[1.75, 1.88]	[2.28, 2.67]
iso measure	[0.50, 0.78]	[1.92, 2.05]

Type of multifractal	Non-epithelial	
	α-min	α-max
maximum measure	[0]	[0.03, 0.44]
summation measure	[1.84, 1.99]	[2.01, 2.42]
iso measure	[0.67, 1.82]	[2.05, 2.08]

B. Mitotic Cell Detection

Mitotic cell tends to have darker colour, and irregular shape. The method of detecting a mitotic cell is displayed in Fig. 4, where a mitotic cell identified by the pathologist and is labelled "M" in Fig. 4(a). An α-threshold, based on summation measure, is applied for detecting mitotic cell. Only pixels with α-value above 55% of the α-range are considered, and they are shown as white clusters in Fig. 4(b). The system scans the binary thresholded α-image and marks the connected components. A connected component is considered as noise if its area is smaller than a predefined threshold. After the removal of the noise, the largest remaining component is usually a mitotic cell. The result of processing the image in Fig. 4(a) using this method is shown in Fig. 4(c).
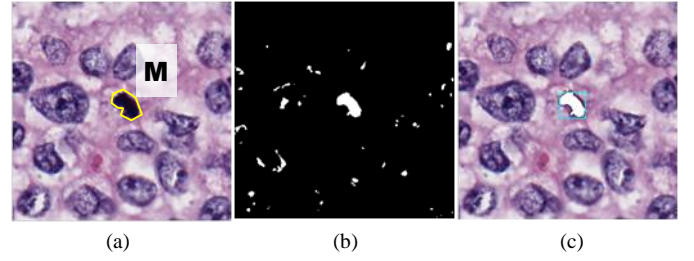

(a)   (b)   (c)

Figure 4.   Process of finding mitotic cell (a) a labelled mitotic cell (b) threshold image (c) detected mitotic cell

C. Nuclear Pleomorphism and Tubule Formation Analysis

Based on Nottingham scoring system [2], [3], the pathologists grade regions of biopsy sections using NP and TF scores between 1 and 3. Table II describes Nottingham grading system for NP and TF. Fig. 5 gives a few image frames with NP and TF scores assigned by the pathologists.

TABLE II.   NOTTINGHAM GRADING SYSTEM FOR NP AND TF

Score	NP	TF
1	nuclei: minimal variation in size and shape	> 75% tubule
2	nuclei: moderate variation in size and shape	10%-75% tubule
3	nuclei: marked variation in size and shape	< 10% tubule

NP = 1, TF = 1   NP = 2, TF = 2   NP = 3, TF = 3

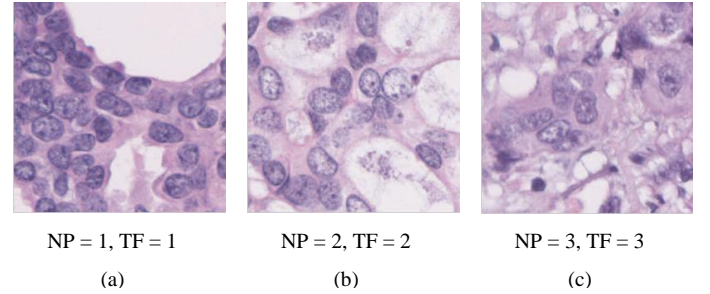(a)   (b)   (c)

Figure 5.   Sample images of Nuclear Pleomorphism and Tubule Formation (a) Score 1 (b) Score 2 (c) Score 3

Petushi et al, Dalle et al, and Tutac et al. analyse the TF scoring with a low resolution global image [6], [7], [8], [9]. This research proposes analysing the TF criterion in high resolution image frame. The advantage of using this technique is that both NP and TF scoring can be estimated together. All four types of multifractal spectrum contain the information of NP and TF as shown in Fig. 6, Table III, and Table IV. The initial goal of our research is to find out which type of multifractal measure returns the best estimate for NP or TF scoring.

TABLE III.   MULTIFRACTAL SPECTRUM FOR NP ANALYSIS

Type of multifractal	α-range of interest	
	from	to
maximum measure	α_0, $f(\alpha_0) = 1$	α-max
inverse minimum measure	α_0, $f(\alpha_0)$ at peak	α_1, $f(\alpha_1) = 1$
summation measure	$\alpha = 2$	α-max
iso measure	α_0, $f(\alpha_0) = 1$	α_1, $f(\alpha_1)$ at peak $1.4 < \alpha_1 < 1.9$

TABLE IV.   MULTIFRACTAL SPECTRUM FOR TF ANALYSIS

Type of multifractal	α-range of interest	
	from	*to*
maximum measure	α-min	α_1, $f(\alpha_1)$ at peak
inverse minimum measure	α_0, $f(\alpha_0) = 1$	α-max
summation measure	α_0, $f(\alpha_0) = 1$	$\alpha = 2$
iso measure	α_0 $\alpha_0 = 0.75 \times$ α-range	α-max
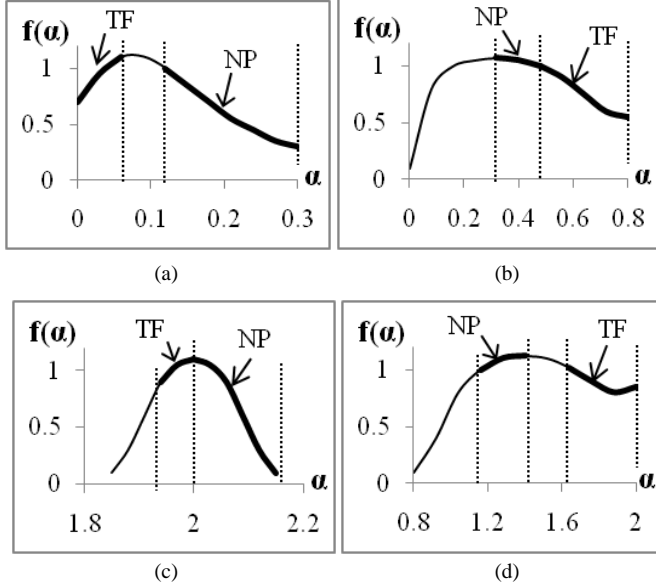
Figure 6.   Multifractal spectrum for NP and TF analysis (a) maximum measure (b) inverse minimum measure (c) summation measure (d) iso measure

The fractal dimension values obtained from the multifractal spectra are used for estimating the NP grade. The nuclei has darker colour hence its intensity value is smaller than other tissue substance. For both maximum measure and summation measure shown in Fig. 7, the second part of the spectrum describes the global intensity distribution of the nuclei. Majority of the nuclei including some of the healthy nuclei and most of the cancer infected nuclei are calculated in the fractal dimension. As labelled in the box in Fig. 7(a) and Fig. 7(b), the spectra for two NP scorings are differentiable in maximum measure and summation measure.
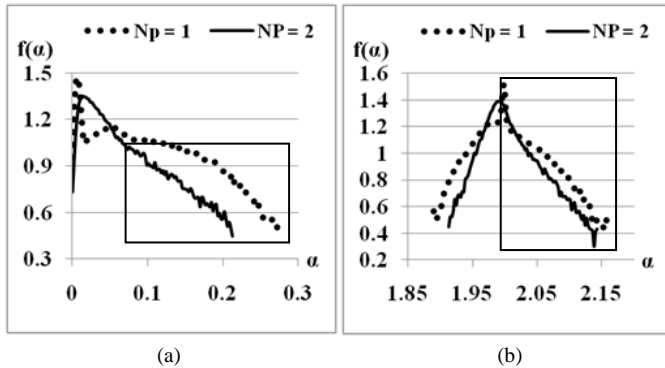

Figure 7.   Fractal spectrum for analysing NP (a) maximum measure (b) summation measure

As highlighted in the box in Fig. 8 (a), the inverse-minimum spectrum shows the difference between two TF scoring. The key information for this spectrum is when it reaches its maximum and to the end of the curve. On the other hand, in Fig. 8(b), the region of interest for iso spectrum, highlighted in the box, is the third quarter of the curve. Each scoring has unique features in both spectra.
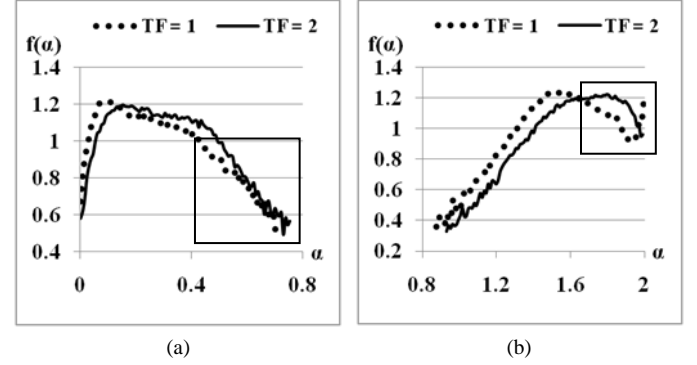

Figure 8.   Fractal spectrum for analysing TF (a) inverse minimum measure (b) iso measure

V.   DISCUSSION

Four histopathological image samples were used for the analysis in this paper; each sample contributes to 250 sub-image frames. In the original histopathological images, the pathologist has labelled 80 regions with NP score and 39 regions with TF score. Each region has a size 1024 by 1024 pixels, and ten sub-image frames are selected from each region. The number of frames used for analysing NP and TF scores are shown in Table V.

TABLE V.   THE NUMBER IMAGE FRAME USED FOR DATA ANALYSIS

Criterion	Score			total
	1	*2*	*3*	
NP	150	190	460	800
TF	150	50	190	390

A. First stage classification process

The thresholds for classifying the epithelial and non-epithelial tissue are dependent on the magnification scale. The magnification scale of the image samples used in this research are ×20.0 and ×40.0. The α-thresholds for classifying non-epithelial type are listed in Table VI.

TABLE VI.   THRESHOLD LIST FOR CLASSIFYING NON-EPITHELIAL TYPE TISSUE

Threshold	Magnification scale	
	×20.0	*×40.0*
α-range of maximum measure	< 0.3	< 0.1
α-range of summation measure	< 0.3	< 0.1
α-min of iso measure	> 0.8	> 1.2

B. Mitotic cell detection

Mitotic cells can be detected with the correct selection of α-threshold and noise threshold. This paper assumes a noise cluster occupies less than 100 pixels and such clusters are removed from the result. In the summation measure, the α-values of the mitotic cell distribute across the second half of the α-range. All potential mitotic cells can be segmented using this feature. After applying the α-threshold process, cluster with the largest number of pixels is consider as the mitotic cell. However, the selection of the α-threshold can affect the outcome. For our analysis, 33 images with mitotic cells were selected, and the comparison chart for different α-threshold is shown in Fig. 9. With a smaller α-threshold, more number of cell nuclei starts to show up as the largest cluster. At an α-threshold is 65% of the α-range, 23 mitotic cells formed the largest clusters in their respective images, but nine mitotic cells that were detected were not the largest cluster in their image frame. In contrast, a higher α-threshold has the risk of not detecting a possible mitotic cell. In the example of Fig. 9, for the α-threshold at 70% of the α-range, 4 mitotic cells were not detected because their sizes were slightly smaller than the pre-defined noise threshold, 100 pixels.
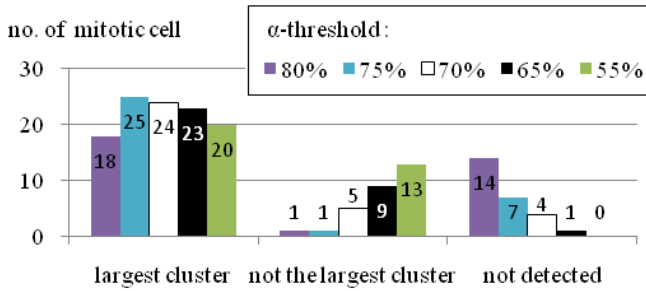

Figure 9.   The comparison of different α-threshold for detected mitotic cell

C. Nuclear Pleomorphism and Tubule Formation scoring

Our research shows that the NP and TF scoring of image sections can be related to certain characteristics of their multifractal spectrum. A simple classification scheme based on multifractal analysis is proposed, and the results of experimental analysis are shown in Fig. 11 and Fig. 12. The section of the multifractal spectrum which varies with NP and TF scores (as previously shown in Fig. 6) can be approximated by a cubic polynomial function, $f^e(\alpha)$ described as follow:

$$f^e(a) = C_3\alpha^3 + C_2\alpha^2 + C_1\alpha + C_0 \qquad (6)$$

where C_3, C_2, C_1, and C_0 are the coefficient of the polynomial function that can be used as the feature vector for classification. An example is shown in Fig. 10.
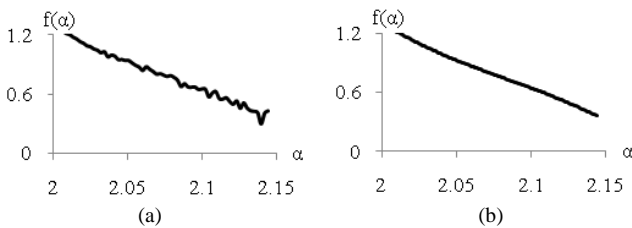

Figure 10. (a) original spectrum (b) polynomial function of $f^e(\alpha)$ = - 201.154403α^3 + 1,257.301618α^2 - 2,625.020288α + 1,831.373506

The reference spectrum for each NP and TF score is calculated based on the average of the multifractal spectrum of images having the same score. The polynomial coefficients are then extracted from the reference spectrum. The multifractal spectrum of a sub-image can then be compared with the reference curve values obtained from the polynomial equation using a distance metric. The classification results for NP and TF scores are shown in Figs. 11 and 12 respectively. Each sample has 200 images frame (as previously described in Table V), and the overall results are presented below. The result for TF scoring using maximum measure is not presented because the cubic polynomial function has error representing the section of the multifractal spectrum.
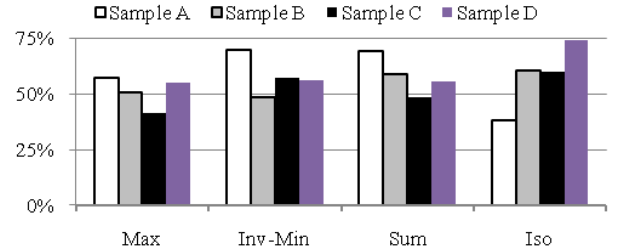

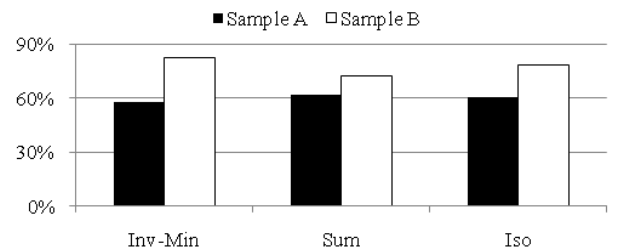Figure 11.   Estimation rate of NP training set

Figure 12. Estimation rate of TF training set

D. Future Work

The result presented in this paper show that multifractal analysis could be a valuable tool in the processing of tissue images for identifying irregularities in the cell structure and in estimating the NP and TF scores. Some of the possible enhancements and future research directions are outlined below.

1) Converting the image into different colour model: Multifractal describes the statistical characteristincs of intensity variations of the image. In this paper, the multifractal spectra are calculated by using only the the red channel of the image frame. Hue model is suggested for color model because it distinguishes the lightness and chroma of the initial colour.

2) Apply genetic algorithm for threshold selection: The thresholds of the classification are manually found for x20.0 and x40.0 magnification scale. 250 sub-image frames are selected from the histopathological image. An automatic threshold selection system, such as using the genetic algorithm, can be useful if threshold for different magnification scale sample is required.

3) Shape detection: Mitotic cell tends to have irregular shape. Majority mitotic cells can be distinguised from their largest pixel area in the thresholded α-image frame. However, as shown in Fig. 9, in some of the images, round shaped nuclei might have the largest area. An automatic shape recognition algorithm to identify and remove regular shapes can improve the detection accuracy of mitotic cells.

4) Increase the number of α-slice: As suggested by Mukundan and Hemsley [23], [24] , increasing the number of subdivisions of the α-range can improve the accuracy of the factal dimensions, but this will also increase the computational complexity. To improve the etimation accuracy of NP and TF scores, it is suggested to improve the number of α-slices only in the relevant portion of the α-range.

VI. CONCLUSION

This research work presented in the paper explored the possibility of using multifractal methods for identifying the statistical characteristics of the image intensity distribution that are important for processing histopathological images. It has been shown that a multifractal decomposition of tissue images could be used for identifying mitotic cells, and also for estimating the NP and TF scores. The proposed multifractal methods could be combined with algorithms for extracting cytological features for effective classification and segmentation of images of biopsy sections.

ACKNOWLEDGMENT

REFERENCES

[1] J. Ferlay, H. Shin, F. Bray, D. Forman, C. Mathers, and D. Parkin, "Globocan 2008 v1.2, Cancer incidence and mortality worldwide: IRAC CancerBase No. 10," Lyon, France: International Agency for Research on Cancer 2010, retrieved from http://globocan.iarc.fr , accessed on 09/09/2011.

[2] R. Cardiff and R. Jensen, "Histological grading of breast cancer," 2011, retrieved from http://ccm.ucfavis.edu/bcancercd/311/grading_diagram.html, accessed on 09/09/2011.

[3] C. Elston and I. Ellis, "Assessment of histological grade," The breast, vol. 13. Churchill Livingstone, Edinburgh, 1998, pp. 356-384

[4] A. Veillard, N. Lomenie, and D. Racoceanu, "An Exploration Scheme for Large Images: Application to Breast Cancer Grading," PCPR, 2010, pp. 3472-3475.

[5] L. George and K. Sager, "Breast Cancer Diagnosis using Multi-Fractal Dimension Spectra," Signal Processing and Communications, 2007. ICSPC 2007. IEEE International Conference, vol., no., pp.592-595, 24-27 Nov. 2007.

[6] A. Tutac, D. Racoceanu, T. Putti, X. Wei, W. Leow, and V. Cretu, "Knowledge-Guided Semantic Indexing of Breast Cancer Histopathology Images," BioMedical Engineering and Informatics, 2008, vol.2, pp.107-112, 27-30 May 2008.

[7] J. Dalle, W. Leow, F. Racoceanu, A. Tutac, and T. Putti, "Automatic breast cancer grading of histopathological images," Engineering in Medicine and Biology Society, 2008. EMBS 2008. 30th Annual International Conference of the IEEE , pp.3052-3055, 20-25 Aug. 2008.

[8] S. Petushi, C. Katsinis, C. Coward, F. Garcia, and A. Tozeren, "Automated identification of microstructures on histology slides," Biomedical Imaging: Nano to Macro, 2004. IEEE International Symposium on , vol., no., pp. 424- 427 Vol. 1, 15-18 April 2004.

[9] S. Petushi, F. U. Garcia, M. M. Haber, C. Katsinis, and A. Tozeren, "Large-scale computations on histology images reveal grade differentiating parameters for breast cancer," BMC Medical Imaging, vol. 6, no. 14, 2006.

[10] J. Beliën, J. Baak, P. van Diest, and A.van Ginkel, "Counting mitoses by image processing in feulgen stained breast cancer sections: The influence of resolution," Cytometry 1997.

[11] T. Kate, J. Beliën, A. Smeulders, and J. Baak, "Method for counting mitoses by image processing in feulgen stained breast cancer sections," Cytometry, vol. 14, pp. 241-250.

[12] C. Demir and B. Yener, "Automated cancer diagnosis based on histopathological images: a systematic survey," Rensseaer Polytechnic Institute, Tech. Rep., 2005.

[13] A. Nedzved, S. Ablameyko, and I. Pitas, "Multiwavelet grading of prostate pathological images," Proc. Int. Conf. Pattern Recognition, 2000, pp. 1500-1503.

[14] H. Jeong, T. Kim, H. Hwang, and H. Choi, "Comparison of thresholding methods for breast tumor cell segmentation," Proc. Of 7th Int. Workshop on Enterprise Networking and Computing in Healthcare Industry, 2005, pp. 392-395.

[15] M. Adawi, Z. Shehab, H. Keshk, and M. Shourbagy, "A fast algorithm for segmentation of microscopic cell images," Proc. of 4th Int. conf. on Information & Communication Technology, 2006.

[16] A. Jadhav, P. Banarjee, K. Chaudhuri, and J. Chatterjee, "Quantitative analysis of histopathological features of precancerous lesion and condition using image processing techniques," Proc. of 19th IEEE Int. Symp. on Computer-Based Medical Systems, 2006, pp. 231-236.

[17] J. Dalle, W. Leow, and D. Racoceanu, "Nuclear Pleomorphism Scoring by Selective Cell Nuclei Detection," IEEE Workshop on Applications of Computer Vision (WACV 2009), Snowbird, Utah, US, December 7-8, 2009.

[18] I. Reljin, B. Reljin, I. Pavlovic, I. Rakocevic, "Multifractal analysis of gray-scale images," Electrotechnical Conference, 2000. MELECON 2000. 10th Mediterranean, vol.2, pp. 490- 493 vol.2, 2000.

[19] I. Relhin and B. Relgin "Fractal geometry and multifractals in analyzing and processing medical data and images," Archive of Oncologt, vol. 10 (4), 2002, pp.283-293.

[20] K. Uma, and K. Ramakrishnan, "Image analysis using multifractals," Proc. of the Intnl. Conf. on Acoustics, Speech, and Signal Processing, vol. 4, 1996, pp. 2188-2190.

[21] T. Stohic, R. Irini, and R. Branimir, "Adaption of multifractal analysis to segmentation of microcalcifications in digital mamaograms," Phusica A, vol. 367, 2006, pp. 494-508.

[22] I. Song, Y. Ji, B. Cho, J. Ku, Y. Chee, J. Lee, M. Lee, I. Kim, and S. Kim, "Multifractal analysis of sleep EEG dynamics in humans," Neural Engineering, 2007. CNE '07. 3rd International IEEE/EMBS Conference on , vol., no., pp.546-549, 2-5 May 2007.

[23] A. Hemsley, R. Mukundan, "Multifractal measures for tissue image classification and retrieval," Multimedia, 2009. ISM '09. 11th IEEE International Symposium on, pp.618-623, 14-16 Dec. 2009.

[24] R. Mukundan, and A. Hemsley, "Tissue image classification using multi-fractal spectra," International Journal of Multimedia Data Engineering and Management (IJMDEM), vol. 1(2), pp. 62-75, 2010.

[25] K. Falconer, Fractal Geometry – Mathematical Foundations and Applications, 2nd ed, Wiley, England 2003

[26] C. Tricot, Curves and Fractal Dimension, Springer, Berlin, 1993

[27] C. Huang, D. Racoceanu, L. Roux, T. Putti, "Bio-inspired computer visual system using GPU and Visual Pattern Assessment Language (ViPAL): Application on breast cancer prognosis," Neural Networks (IJCNN), The 2010 International Joint Conference, pp.1-8, 18-23 July 2010